FTDT investigations for fabrication of sub-wavelength metal wire-grid polarizer and quarter waveplate

C. COTIRLAN-SIMIONIUC*, C. LOGOFATU, G. IORDACHE, A. RIZEA[a], D. V. URSU[b], C. MARIN[b]
National Institute of Materials Physics, P.O.Box MG-7, RO-077125 Magurele, Romania
[a]*ProOptica S.A., 67, Gh.Petrascu St., RO-745081, Bucharest, Romania*
[b]*Institute of Optoelectronics S.A., 67, Gh.Petrascu St., 401 room, RO-745081, Bucharest, Romania*

Ultracompact polarization components modeled and analyzed with Finite Difference Time Domain Photonics Simulation Software (FTDT) are: a wire-grid linear polarizer and a quarter waveplate for infrared (IR) domain. They will be integrated into a polarization state analyzer (PSA). The components will be manufactured with metamaterials (MTMs). These are composite materials consisting of artificial meta-atoms, *i.e.* conductive nano- or micro-structures regularly arranged in a dielectric or semiconductor matrix. These conductive structures are made-up smaller than the wavelength of the radiation work. MTMs show extraordinary electromagnetic properties, typically not found in nature, such as negative refractive index. They increase the interaction between radiation and matter. The use of optical polarization components in IR imaging systems dedicated to difficult conditions of visibility is a must, as it allows improving performance and reducing the dimension of optoelectronic devices used in air, car and naval navigation. We will focus on developing the components for applications of imaging polarimetry in long-wave infrared (LWIR) range.

(Received November 10, 2015; accepted November 25, 2016)

Keywords: Polarizer, Quarter-wave plate, Metamaterials, Polarimetry

1. Introduction

The goal of this paper is to investigate the FTDT software possibilities of modeling and analyze for subwavelength IR devices that enables imaging polarimetry. The polarization information can help to discriminate thermal objects from natural background in numerous remote sensing navigation applications [1].

Imaging polarimetry measures the polarization states of light from all the points of the scene. A simplified approach uses a rotating waveplate followed by a fixed polarizer with several sequential images taken to characterize the Stokes parameters across a scene. The polarization state of light can be completely described by four Stokes parameters. The first Stokes parameter, S_0, represents the total optical intensity. The second Stokes parameter, S_1, represents the preference of the recorded optical signal for horizontal polarization versus vertical polarization. The third Stokes parameter, S_2, represents the preference of the recorded optical signal for linear polarization oriented along 45° versus 135° measured with respect to the horizontal direction. The fourth Stokes parameter, S_3, represents the preference for right-circular polarization versus left-circular polarization.

Almost all the photodetectors available now are polarization insensitive, thus a combination of polarizing elements, *e.g.,* linear polarizer (LP), quarter waveplate (QWP) and photodetectors is needed to measure the polarization content of light. LP for LWIR are made by patterning nano-scale metallic grids on an IR transparent substrate [2]. A QWP designed to match the spatial division of the IR image is the key element in a complete polarimeter [3]. Subwavelength structured gratings lead to an effective index that is dependent on the incident polarization. This effect is known as form birefringence and can be utilized to provide a waveplate. Subwavelength gratings have been shown to provide a birefringent dispersion that is amenable to providing an achromatic phase retardance [4]. The metamaterials (MTM) for making optical components, *e.g.* ultrathin flat lenses [5,6] polarization-selective filters [7], frequency selective surfaces [8], couplers [9], gives new insights in many applications. With MTM can be obtained optical components for near-field or far-field applications with an optical resolution beyond the diffraction limit. The optical surfaces with micro- and nanostructures can be evaluated so as to identify the most promising components for high efficiency thermal imaging. This paper examines the design of a QWP for operation over a spectral region slightly more limited than LWIR (8÷12 μm). The LWIR applications require LP with low insertion loss, high extinction ratios, a broad wavelength range for the incident waves, and QWP with strong anisotropy and high transparency for compact size systems with efficient packaging.

2. Design approach

LP is made by patterning nano-scale metallic grids on a LWIR transparent substrate [10]. The QWP or phase retarder is made currently by deeply etching the nano-scale structure on Ge substrate, and then deposition of Ag in the resulted grooves [11]. The QWP has been designed

employing transparent photonic MTMs of remarkably strong anisotropy. The QWP is far more efficient at IR wavelengths than usual bulk waveplates and are shown to be compact down to sub-wavelength dimensions.

2.1. Wire-grid polarizer simulations

A suspended perfect conductor subwavelength wire-grid in air would be ideal as LP, but it is mechanically inpractical to fabricate such long and thin wires. We should choose a low refractive index substrate to support the metallic subwavelength-period wire grid, but common IR optical materials with high transmission and low index on broadband range are water soluble. Therefore, we have chosen to investigate GaAs with refractive index n=3.28@10μm as IR substrate for LP. A numerical survey of the transmission of TM and TE fields was done for various wire-grid period, metal thicknesses, and wavelengths using OptiFTDT Designer. In order to make a good metal grid polarizer, the period of the metallic grid must be at least one order of magnitude less than the incident wavelength [12].

The wire-grid LP configuration is shown in Fig. 1.

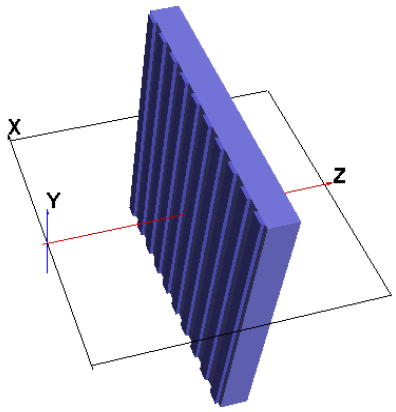

Fig. 1. 3D Layout model for linear polarizer

2.2. Wideband quarter waveplate simulations

It was previous clarified that stratified metal-dielectric metamaterials (SMDMs) are transparent and remarkably anisotropic media in a wide wavelength range [13]. A typical QWP has high-index substrate for strong birefringence. The structure of a SMDM is schematically drawn in Fig. 2 below LP. It consists of alternating metallic (gray) and dielectric or semiconductor (blue) layers. The periodicity of the layered medium is fairly shorter than the incident wavelength, thus the description uses effective optical indices [13]. We concentrate on the case that the incident light normally illuminates on the *xy* plane. As typical case, we evaluated the modified SMDMs. The width of metallic layers (Ag) at the bottom (z=-d) is narrower by 20% than that at the top (z=0). The chosen semiconductor is Ge with n=4.03@10 μm for substrate.

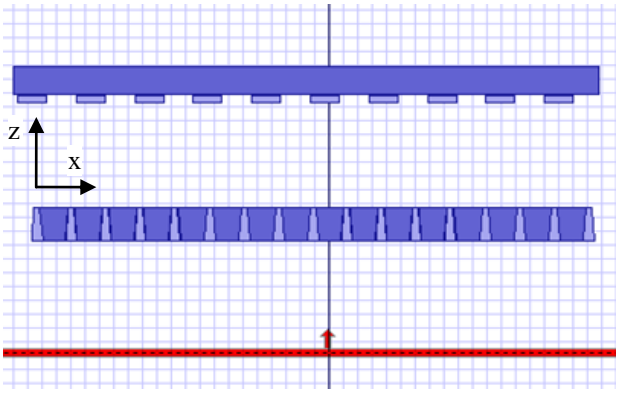

Fig. 2. 2D Layout model for PSA

The simplified structure of PSA is shown in Fig. 2 with the rectangular transverse wave, 5 μm half width.

3. Theoretical modeling

The finite difference time-domain (FDTD) method, a powerful and accurate method for finite size structure, was chosen to simulate and design the polarizer and QWP integrated in PSA. In an earlier publication were presented results for several metals used in making wire-grid for IR polarizer [10]. It was found that Au has preferred optical performances on extended region: MWIR and LWIR. But, we search for simplification and integration of the technologies for achieving the LP and the QWP with a single metal. So, we chosen silver (Ag) for wire-grids because Ag has the most linear permittivity on the widest range of wavelengths [14], and his plasmonic features are the best [15]. Finally, it is cheaper than Au.

Fig. 3 shows the simulation results obtained using OptiFDTD software for wave propagation with λ=10 μm in LP. The plotted field is the real part of E_y and H_x.

The position of wire-grid frontline is at z=9.5.

The simplest polarimetric system uses a single serial processing channel with rotating waveplate relative to polarizer and detector array [16]. The most complex one uses four separate channels with parallel processing [1] or integrating of four PSA (composed of the waveplate and polarizer) for each pixel of the focal plane array [12]. The last system has the advantage of eliminating temporal fluctuations between adjacent pixels, but introduce signal degradation due to the effects of diffraction and interference between pixels. In passive techniques for IR broadband one-dimensional polarimetric imaging is used a single polarizer filter. For differential polarimetry two polarization filters are used and two separate channels of analysis, and for three or full dimensional polarimetry up to 4 channels of polarization filters and waveplates are involved.

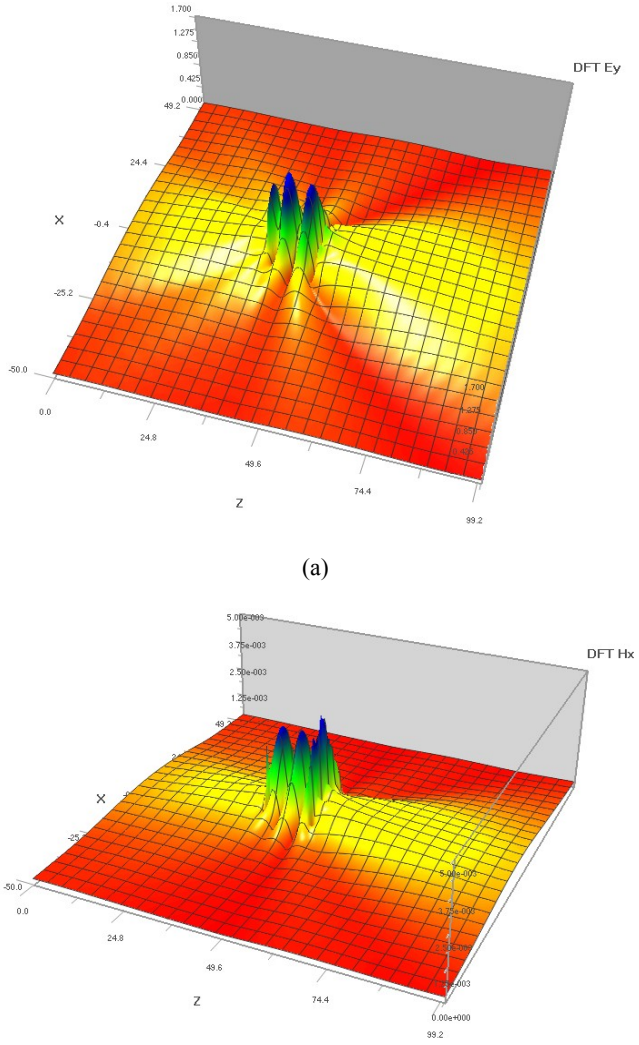

(a)

(b)

Fig. 3. Distribution of the optical field with λ=10μm by the LP simulated with software OptiFDTD. The plotted field is the real part of E_y (a) and H_x (b). LP is positioned at z=49 μm.

It is assumed that all the metal wire-grids are sufficiently long along the z direction so that a two dimensional FDTD method can be used to simplify the simulation.

The perfectly matched layers (PML) [17] were along the y direction. The boundaries along the x direction were confined with the periodic boundary conditions (PBC) due to the periodicity of the wire-grids.

The plane wave normally propagates to the metal wire-grid. The dielectric function for metal, Ag, was described by the Lorentz-Drude model [18]. The Lorentz-Drude model is a more general dispersive case. Most of the dispersive effected can be fitted into Lorentz-Drude model.

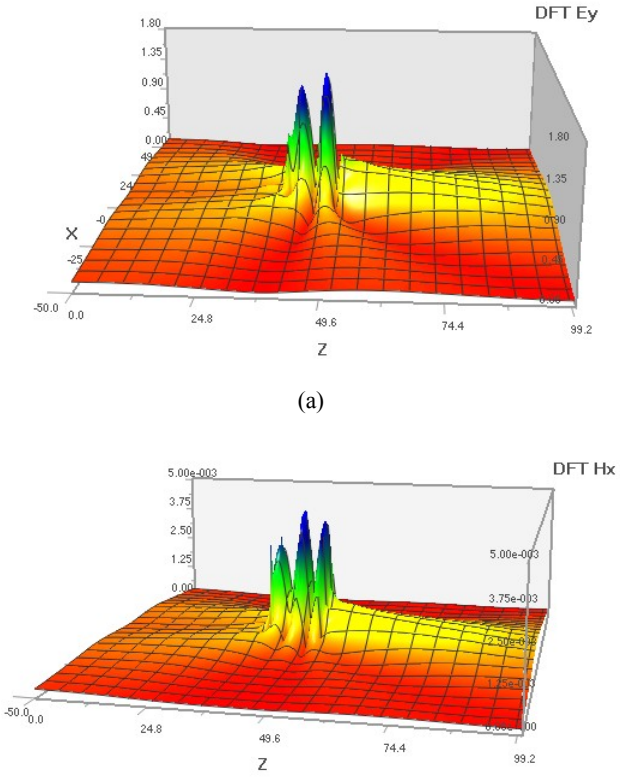

(a)

(b)

Fig. 4. Distribution of the optical field by the PSA simulatted with software OptiFDTD (LP at z=45 μm and QWP at z=50 μm). The plotted field is the real part of Ey (a) and the H_x (b).

The optical system modeled to determine phase delay of diffractive waveplate comprisis: an IR source in conjunction with a monochromator, an IR collimating lens, an IR polarizer and an iris used to ensure that only the QWP is illuminated. The QWP can be mounted on a rotation stage to allow measurement of the output with respect to its angular position. An analyzing polarizer followed the QWP and a final lens should be used to focus the output on an IR detector. This system for QWP characterization can be modeled using Jones matrices.

On the other hand, Mueller matrices are often used for systems that are not fully polarized. While this is true for a general source, the use of a first polarizer before QWP allows for the use of a simpler Jones matrix model. The Mueller matrix of a general anisotropic sample is a function of both the azimuth angle and the angle of incidence [19].

However, for a fixed angle of incidence one can relate the Mueller matrices at different azimuth angles by using Mueller matrix transformations for optical elements. This fact allowed us to take advantage of information overlap between intensities recorded for various azimuth angles for a fixed angle of incidence.

The information overlap between intensities recorded for different angles of incidence is still unexploited. It is likely that combining this information will improve the robustness of the approach.

This fact is not possible within the framework of the Mueller matrix as there are no general relations to relate the Mueller matrices of different angles of incidence.

An alternative approach might be to work directly with the optical matrix [20] that is composed of permittivity tensor, permeability tensor and rotation tensors. The equation (1) shows the basic model:

(1)

where a and b are the horizontal and vertical polarizations, respectively, Φ_{wp} is the waveplate phase delay and θ is the rotation angle of the waveplate.

The subscripts refer to the individual elements in the system; *pol* for the polarizer, *ana* for the analyzer and *wp* for waveplate; a_{wp} and b_{wp} are diattenuation parameters. In order to properly model the system, two alterations were made to Equation (1). First, a rotation was added to the analyzer to compensate for a possible angular misalignment. Second, a small sinusoidal modulation of the input has compensated the lateral misalignment of the QWP. Since, the outputs of the Jones matrix model are field quantities, these results were squared to provide a value consistent with the intensity measurement made by the detector. The output of the system is taken at several angular positions of the QWP. In addition, the output of the system can be measured without the analyzer in place.

Theoretically, this would have provided no change with rotation of the QWP.

However, the practical waveplate can exhibite an appreciable amount of linear diattenuation at certain wavelengths. Linear diattenuators have a transmission efficiency that is dependent on the incident polarization. A technique to measure linear diattenuation and retardance spectra of IR materials in transmission, compensation for systematic errors, and the utility for the calibration of retarders and polarizers are described in [21] for several wavelengths across the spectral region of interest.

The simulated phase retardation Φ_{wp} for QWP is shown in Figure 6 along with the extinction ratio (E_x/E_y) or TM/TE (ratio between transverse magnetic mode with electric-field vector perpendicular to the wire and transverse electric mode with electric-field vector parallel to the wire) for LP. The geometry parameters for LP are substrate thickness D=1.2 μm, period p=2 μm, height of metal gratings h=250 nm and the duty cycle of 0.5. The enhancement of the TM polarization with growth of grid height is counterbalanced by lowering the transmission efficiency with increasing of the width for grating lines.

The combination of these effects leads to the improvements in polarization properties along with increasing the width of the metallic gratings [10]. For practical waveplate, a small error in the duty cycle of QWP causes a large change in the phase delay, particularly at the longer wavelengths. We chose the following geometrical parameters for QWP: substrate thickness of 1.2 μm, Ag/Ge 200/800 nm width with 20% variation of metallic layers width from top to bottom and a duty cycle Ag/Ge of 0.8.

4. Results

The best Ey distribution is obtained for 0 μm distance between components at simulation with central wavelength of λ=10 μm (Figs. 5, 6). In practice, the distance between the two components is now the glue distance, which usually is 10 μm. If the distance between PSA components increases, then there is a slight sinusoidal modulation of Ey amplitude in the range 1.8-2.2 due to cross-talk over proximity to the grids from both components. The analysis indicates variation in extinction ratio as the separation increases between the Ge substrate and the wire-grid on GaAs. If using a bare QWP substrate, the extinction ratio oscillates as the wavelength increases.

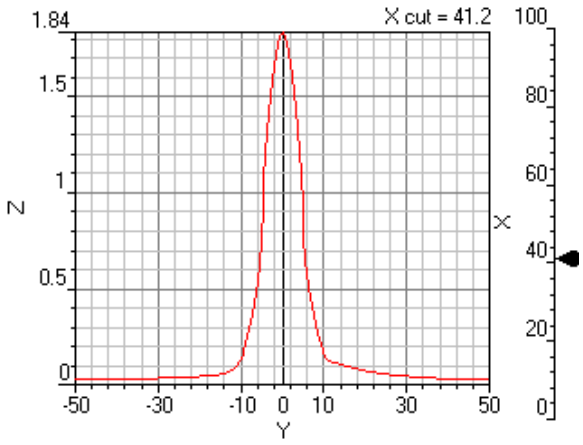

Fig. 5. Distribution of the optical field by the PSA simulatted with software OptiFDTD (LP input surface is at z=45 μm. Distance between LP output side and QWP input surface is 0 for this simulation). The plotted field is the real part of Ey with x cut.

In computing the fields, the SMDM is assumed to be infinite along the *y* axis. The incident region contains both incident and reflected lights; however, a small reflection, which is at most several percents, hardly affects the electric fields of incidence.

We can optimize the architecture performance for device using additional AR layers under each component substrate, so that higher coupling efficiency can be achieved. With AR layers, the field distribution and coupling efficiency can both be improved. The oscillation frequency decreases as the separation between the two devices increases.

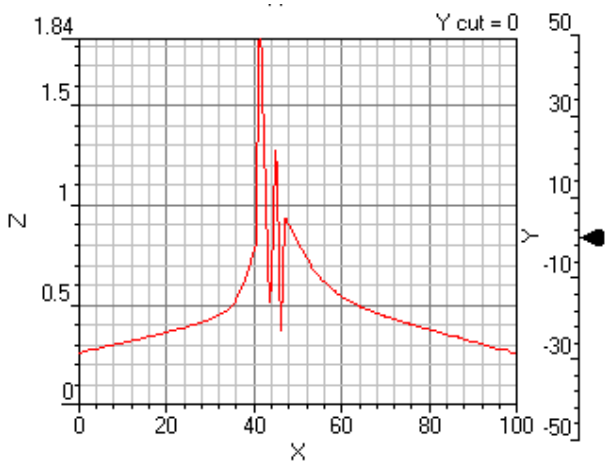

Fig. 6. The plotted field is the real part of Ey with y cut.

Depositing an antireflective (AR) coating on the Ge substrate reduces apparent the extinction ratio oscillation and losses.

The AR coating should be patterned to the areas without gratings. Depositing an AR coating on the patterned areas of the GaAs and Ge substrates is unfeasible because the AR coating will change the optical characteristics of the gratings.

In addition, deposition rates can not be controlled well for vertical walls and sometimes deposition may not occur.

The thickness of the AR coating could exceed the open lines of the grating. On the other way, the transmission for the light entering the grating substrate in 8÷12 μm spectral range is 55% for GaAs and 42% for Ge without AR coatings.

To solve this situation is desirable to fine tune the design of the grating with the wire-grid polarizer in proximity to the QWP device. Also, an additional loss is incurred at the output interface of the Ge substrate due to Fresnel reflections. Resultant transmission losses, on the order of 4% per interface, can be reduced considerably by the use of index-matching materials.

We note that the transmittance is slightly lower in the 20% top reduced SMDM than in the classical SMDM, but the optical loss in the modified structures is quite suppressed.

It has thus been confirmed that SMDMs are quite robust in structural modifications and strong candidates for ultracompact waveplates (UCW) [11].

These UCW already can be integrated with other optical flat, free aberrations components on a single chip. It is a trend favored by implanting miniaturized photonic systems.

The results of OptiFTDT analysis for LP extinction ratio and QWP retardance are shown in Fig. 7.

The Ag wire-grid LP has a very good optical polarization performance on a relative broadband wavelength range from 9.5 to 11.5 μm. The extinction ratio of simulated LP were larger than 100 over 10.5 to 11.5 μm range. The theoretical results for retardance have a decreasing slope versus wavelength with an average phase delay of 90º.

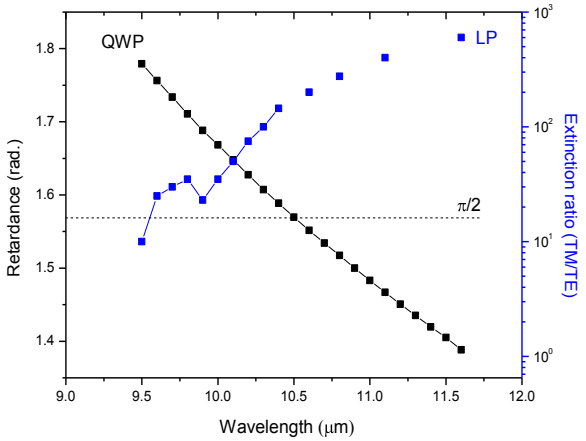

Fig. 7. Extinction ratio for LP: Ag/GaAs, D=1.2 μm, h=0.25 μm t=1 μm, p=2μm, the retardance for QWP with thick =1.2 μm, Ag/Ge width=200/800 nm.

The work is also focused on transmission of light through aligned LP and QWP. Figure 8 represents the PSA transmission for TM mode. Combining the Fresnel reflections with the simulated transmission of the grating should obtain the real transmission curves.

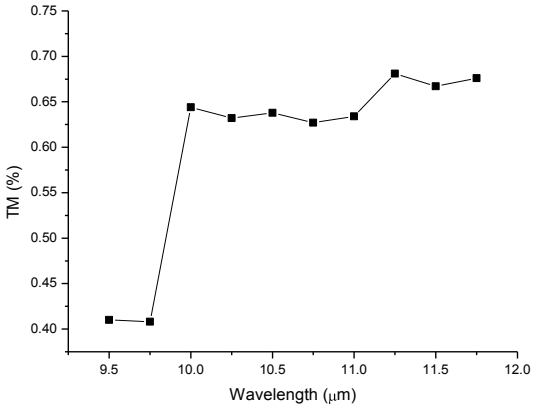

Fig. 8. Transmission through ASP (LP and QWP) for TM. The distance between LP output side and QWP input surface is 0.

The transmitted TM indicates that ASP (LP on GaAs and QWP on Ge) can perform across the 10÷12 μm range, better to longer wavelengths. Thus, while GaAs has a better transmission, but cleaves easily, Ge has the highest density of the IR-transmitting materials, and it is very popular for systems operating in LWIR region. Ge is the subject to thermal runaway, the hotter it gets, the more the absorbtion increases. Pronounced transmission degradation starts at about 100°C and begins rapidly decreasing between 200°C and 300°C, resulting in possible catastrophic failure of the optic. However, its high index is desirable for the design of IR optics that might not otherwise be possible.

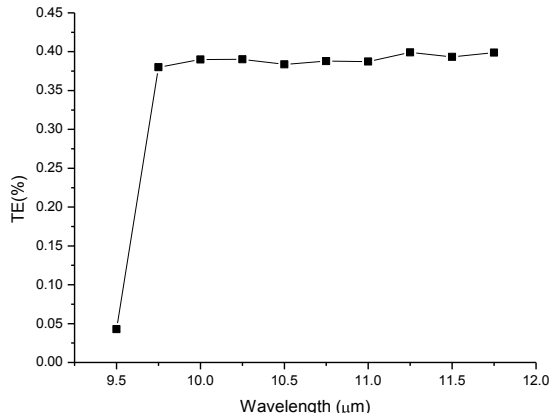

Fig. 9. Transmission through ASP (LP and QWP) for TE

Fig. 9 shows a great value of the (TE) irradiance, that requires the use of IR antireflection coatings on the unstructured surfaces. If TE becomes small enough, below 1%, then extinction ratio increases adequately.

5. Conclusions

The OptiFTDT design is performed for a PSA device in the LWIR range. A wire-grid LP and a diffractive QWP based on one-dimensional subwavelength Ag gratings are modeled on GaAs substrate, respectively Ge substrate. For LP, extinction ratios greater than 100:1 are obtained for wavelengths of 10.5 to 11.5 μm.

The QWP is not achromatic, because the retardance is decreasing almost linearly with the wavelength.

The use of OptiFTDT Analyzer shows a design with good transmission without AR coatings over the 10÷11.5μm spectral band. However, the AR coatings are required for reducing the irradiance. The results from the analyze of integrated PSA indicate that the assembly LP and QWP with each component on own substrate and stacking them is too sensitive to cross-talk.

This cross-talk is the product of diffraction from the periodic structures defined by the wire-grid of LP and wire-grid of QWP. The diffracted light bleeds into far field on the adjacent pixels of a detector array or into free space.

This could lead to a false-positive target in the polarimetric image. An integrated approach provides a better alternative in the thermal imager without AR coatings between IR components. But, in this case the wire-grid for LP could be deposited on QWP substrate as part of the PSA device fabrication process. The birefringent waveplate should be fabricated in its own substrate and aligned with the grating facing the detector active area. The integrated PSA should have the AR coatings on both outer surfaces. The QWP input side is almost flat, because the Ag is deposited in grooves until to surface. The AR coating for LWIR could be deposited between the wire-grides of LP directly on substrate only for applications that require maximum performances.

Acknowledgements

This work was supported by PN II Partnership Program, contract no. 277/2014, under the Ministry of Education and Scientific Research, Romania.

References

[1] J. S. Tyo, D. L. Goldstein, D. B. Chenault, J. A. Shaw, Appl. Opt. **45**(22), 5453 (2006).
[2] Z. Wu, P. E. Powers, A. M. Sarangan, Q. Zhan, Opt. Lett. **33**(15), 1653 (2008).
[3] K. P. Gurton, R. Dahmani, G. Videen, US Army Research Laboratory Report, ARL-TR-3240 (2004).
[4] M. W. Kudenov, E. L. Dereniak, L. Pezzaniti, G. R. Gerhart, Proc. SPIE **6972**, 69720K (2008).
[5] A. W. Lohmann, A. Pe'er, D. Wang, A. A. Friesem, J. Opt. Soc. Am. A. **17**(10), 1755 (2000).
[6] N. Yu, F. Capasso, Nat. Mat. **13** doi: 10.1038/NMAT3839 (2014).
[7] S. Sun, Q. He, S. Xiao, Q. Xu, X. Li, L. Zhou, Nat. Mat., doi: 10.1038/NMAT3292 (2012).
[8] R. Mittra, Proceedings of the IEEE **76**(12), 1593 (1988).
[9] Z. Zhou, L. Yu, Optical Engineering **52**(9), 091708 (2013).
[10] W. Guo, Z. Li, H. Gao, L. Xia, L. Shi, Q. Deng, C. Du, Proc. of SPIE **8759**, 87593I-1 (2013).
[11] M. Iwanaga, Appl. Phys. Lett. **92**, 153102 (2008).
[12] S. A. Kemme, A. A. Cruz-Cabrera, R. R. Boye, T. Carter, S. Samora, C. Alford, J. R. Wendt, G. A. Vawter, J. L. Smith, 2006, Sandia Report SAND2006-6889.
[13] M. Iwanaga, Opt. Lett. **32**, 1314 (2007).
[14] OptiFDTD Material Library, Finite Difference Time Domain Photonics Simulation Software, Optiwave Co. (2008).
[15] G. Naik, A. Boltasseva, SPIE Newsroom, doi: 10.1117/2.1201201.004077 (2012).
[16] J. Scott Tyo, Bradley M. Ratliff, James K. Boger, Wiley T. Black, David L. Bowers, Matthew P. Fetrow, Opt. Express **15**(23), 15161 (2007).
[17] J. P. Beranger., J. Comput. Phys. **114**, 185 (1994).
[18] A. D. Rakic, A. B. Djurisic, J. M. Elazar, M. L. Majewski., Appl. Opt. **37**, 5271 (1998).
[19] S. Tripathi, K. C. Toussaint, Jr, Opt. Express **17**(24), 21396 (2009).
[20] R. M. A. Azzam, N. M. Bashara, "Reflection and transmission of polarized light by stratified planar structure" in *Ellipsometry and polarized light,* North Holland, Amsterdam, Chap. 4 (1989).
[21] D. B. Chenault, R. A. Chipman, Appl. Opt. **32**(19), 3513 (1993).

*Corresponding author: costel.cotirlan@infim.ro